Applied Microbiology and Biotechnology (2018) 102:3879–3892
https://doi.org/10.1007/s00253-018-8889-5

MINI-REVIEW

Elementary processes for the entry of cell-penetrating peptides into lipid bilayer vesicles and bacterial cells

Md. Zahidul Islam[1,2] · Sabrina Sharmin[2] · Md. Moniruzzaman[2] · Masahito Yamazaki[2,3,4]

Received: 29 December 2017 / Revised: 21 February 2018 / Accepted: 23 February 2018 / Published online: 9 March 2018

Abstract

Cell-penetrating peptides (CPPs) can translocate across the plasma membrane of living eukaryotic cells and enter the cytosol without significantly affecting cell viability. Consequently, CPPs have been used for the intracellular delivery of biological cargo such as proteins and oligonucleotides. However, the mechanisms underlying the translocation of CPPs across the plasma membrane remain unclear. In this mini-review, we summarize the experimental results regarding the entry of CPPs into lipid bilayer vesicles obtained using three methods: the large unilamellar vesicle (LUV) suspension method, the giant unilamellar vesicle (GUV) suspension method, and the single GUV method. The advantages and disadvantages of these methods are also discussed. Experimental results to date clearly indicate that CPPs can translocate across lipid bilayers and enter the vesicle lumen. Three models for the mechanisms and pathways by which CPPs translocate across lipid bilayers are described: (A) through pores induced by CPPs, (B) through transient prepores, and (C) via formation of inverted micelles. Both the pathway of translocation and the efficiency of entry of CPPs depend on the lipid composition of the bilayer and the type of CPP. We also describe the interaction of CPPs with bacterial cells. Some CPPs have strong antimicrobial activities. There are two modes of action of CPPs on bacterial cells: CPPs can induce damage to the plasma membrane and thus increase permeability, or CPPs enter the cytosol of bacterial cells without damaging the plasma membrane. The information currently available on the elementary processes by which CPPs enter lipid bilayer vesicles and bacterial cells is valuable for elucidating the mechanisms of entry of CPPs into the cytosol of various eukaryotic cells.

Keywords CPPs · Transportan 10 · Oligoarginine · Large unilamellar vesicle · Giant unilamellar vesicle · Pore · Prepore · Leakage · Bacterial cells

Introduction

Charged molecules such as ions and proteins cannot pass through the lipid bilayer regions of the plasma membrane of various cells because the core of the lipid bilayer is composed solely of hydrocarbon chains and thus has a low dielectric constant (Hille 1992). Therefore, various transport systems have developed in the plasma membrane of eukaryotic cells over a long evolutionary period. Ion transporters, ion channels (Hille 1992), and endocytosis (Doherty and McMahon 2009) are the major transport systems. However, cell-penetrating peptides (CPPs), which are highly positively charged peptides, can independently enter the cytosol of living eukaryotic cells. CPPs can therefore be used for the intracellular delivery of biological cargo such as proteins and oligonucleotides (Magzoub and Gräslund 2004; Zorko and Langel 2005; Madani et al. 2011; Bechara and Sagan 2013; Stanzl et al. 2013). Most CPPs can be generally categorized into two types: arginine-rich CPPs (Vivès et al. 1997; Futaki et al. 2001; Richard et al. 2003), such as the human immunodeficiency virus Tat protein-derived peptide Tat (48–60) (GRKKRRQRRRPPQ), oligoarginine CPPs (R_n, e.g., R_9),

✉ Masahito Yamazaki
yamazaki.masahito@shizuoka.ac.jp

[1] Present address: Department of Biotechnology and Genetic Engineering, Jahangirnagar University, Savar, Dhaka 1342, Bangladesh

[2] Integrated Bioscience Section, Graduate School of Science and Technology, Shizuoka University, Shizuoka 422-8529, Japan

[3] Nanomaterials Research Division, Research Institute of Electronics, Shizuoka University, 836 Oya, Suruga-ku, Shizuoka 422-8529, Japan

[4] Department of Physics, Graduate School of Science, Shizuoka University, Shizuoka 422-8529, Japan

and amphipathic CPPs, such as penetratin, transportan (TP), transportan 10 (TP10) (a truncated analogue of TP; AGYLLGKINLKALAALAKKIL), and pVEC (Pooga et al. 1998; Soomets et al. 2000; Pooga et al. 2001; Elmquist et al. 2001; EL-Andaloussi et al. 2005).

Several pathways have been proposed for the entry of CPPs into eukaryotic cells, including various endocytic pathways (such as clathrin-mediated endocytosis and macropinocytosis) (Doherty and McMahon 2009), and direct translocation across the plasma membrane (Magzoub and Gräslund 2004; Zorko and Langel 2005; Madani et al. 2011; Bechara and Sagan 2013; Stanzl et al. 2013; Pisa et al. 2015). The pathways by which CPPs enter the cytoplasm have been investigated by studying the colocalization of CPPs with markers of endocytic pathways and by determining the effects of inhibitors of endocytic pathways. There are several inhibitors of clathrin-mediated endocytosis, such as chloroquine (Madani et al. 2011), chlorpromazine (Duchardt et al. 2007), bafilomycin (Wang et al. 2016), and low temperature (4 °C). Macropinocytosis inhibitors include amiloride (Wadia et al. 2004), 5-(*N*-ethyl-*N*-isopropyl) amiloride (EIPA) (Duchardt et al. 2007), and cytochalasin D (Madani et al. 2011). If an inhibitor of a specific endocytic pathway decreases the efficiency of entry of a CPP, we can consider that this specific endocytic pathway is the main entry pathway for this CPP, but if no inhibitor decreases the efficiency of entry of a CPP, the main pathway for this CPP may be direct translocation across the plasma membrane. For example, Tat (48–60) enters cells via clathrin-mediated endocytosis (Richard et al. 2003), although results obtained using a knockdown of clathrin-mediated endocytosis (in BHK21-tTA/anti-clathrin heavy chain cell line) and a knockout of caveolin-mediated endocytosis (in cav-1-KO mouse endothelioma cell line) suggest that Tat peptide enters via direct translocation across the plasma membrane (Ter-Avetisyan et al. 2009). It was also reported that TP10 enters via direct translocation of the plasma membrane (Soomets et al. 2000). Oligoarginine is internalized via clathrin-mediated endocytosis (Richard et al. 2003; Fischer et al. 2004), but in some cases can be internalized via direct translocation across the plasma membrane (Rothbard et al. 2005; Wang et al. 2016). Regardless of the mechanism, CPPs must translocate across the lipid bilayer region of the plasma membrane (including the endosomal membrane) to enter the cytosol of cells. It has been shown that CPPs transfer with low efficiency from the endosomes to the cytosol if they enter cells via clathrin-mediated endocytosis (El-Sayed et al. 2009; Qian et al. 2015).

In this mini-review, we focus on research into the entry of CPPs into lipid bilayer vesicles and bacterial cells. The physicochemical properties of lipid bilayer vesicles are similar to those of the plasma membrane of cells and therefore various studies have been conducted using vesicles, since lipid bilayers are excellent models of plasma membranes (Lipowsky and Sackmann 1995; Baumgart et al. 2003; McLaughlin and Murray 2005; Bigay and Antonny 2012; Islam et al. 2014b). Two types of unilamellar vesicles comprising a single lipid bilayer are typically used for research: large unilamellar vesicles (LUVs) with a diameter of 50 nm–1 μm (100–300 nm for most uses) and giant unilamellar vesicles (GUVs) with a diameter larger than 1 μm (10–40 μm for most uses). Research on the entry of CPPs into lipid bilayer vesicles can be categorized into three groups based on the experimental method used: (1) the LUV suspension method, (2) the GUV suspension method, and (3) the single GUV method. We describe these methods in the following sections.

The LUV suspension method

The LUV suspension method has been extensively used for investigating the interactions of compounds such as peptides/proteins with lipid bilayers. In this method, the compound is mixed with many LUVs (e.g., ~ 10^{11} LUVs with a diameter of 200 nm in 1 mL buffer to provide a 50 μM lipid concentration). The ensemble averages of physical properties of all the LUVs in this suspension are then measured using various biophysical and physicochemical techniques, such as fluorescence spectroscopy, light scattering, nuclear magnetic resonance, electron spin resonance, and X-ray scattering (Fig. 1a). A common experimental method using such suspensions is to measure peptide-induced leakage of the internal contents of the LUVs, such as water-soluble fluorescent probes (i.e., the diffusion of the internal contents from the LUV lumen to the outside aqueous solution). For example, TP10 induces the leakage of water-soluble small fluorescent probes (such as carboxyfluorescein and calcein) from the inside of LUVs comprising palmitoyl-oleoyl-phosphatidylcholine (POPC) or a palmitoyl-oleoyl-phosphatidylglycerol (POPG)/POPC mixture (Bárány-Wallje et al. 2007; Yandek et al. 2007). The rate of total leakage from all LUVs in a suspension increases with an increase in TP10 concentration (e.g., ~ 50% leakage at 20 min for 100 μM TP10 for POPC-LUVs). Yandek et al. also investigated the mode of TP10-induced leakage using fluorescence ANTS/DPX assays (Ladokhin et al. 1995) and found that the leakage of fluorescent probes is "graded" (Yandek et al. 2007). The authors analyzed these data quantitatively based on the assumption that the leakage of the fluorescent probes occurred during the translocation of TP10 across the lipid bilayer (Yandek et al. 2007, 2008). Penetratin induced leakage from LUVs that mimic the lipid composition of the late endosomal membrane (23% leakage at 30 min for 20 μM penetratin), but R_9 did not induce significant leakage from the same LUVs (1% leakage at 30 min for 20 μM R_9) (Qian et al. 2016).

However, the LUV suspension method has several disadvantages. First, several factors (such as pore formation, membrane fusion, rupture, and fragmentation of the liposomes) can

likely induce leakage of the internal contents (such as water-soluble fluorescent probes) from LUV lumens. We cannot observe directly the structure of each LUV in buffer in real time, although LUVs fixed by negative staining and LUVs in vitrified ice can be observed using electron microscopy (EM) and cryo-EM, respectively (Yamazaki et al. 1994). Therefore, we cannot identify the main cause of compound-induced leakage using the LUV suspension method (Yamazaki 2008). Furthermore, only ensemble average values of physical parameters of the LUVs are obtained from a large number of LUVs in a suspension (Fig. 1a) (Yamazaki 2008). Moreover, each LUV is in a different elementary process of the compound-induced structural change of the vesicle, and hence, we observe the average values of the physical parameters of the different elementary processes. This averaging increases ambiguity of the observed values. Therefore, we cannot obtain detailed information on the elementary processes of compound-induced leakage using the LUV suspension method (Yamazaki 2008).

The internalization or entry of fluorescent probe-labeled CPPs into LUVs has been measured using various methodologies such as energy transfer (Drin et al. 2001; Thorén et al. 2004; Persson et al. 2004), isothermal titration calorimetry (Binder and Lindblom 2003), mass spectrometry (Walrant

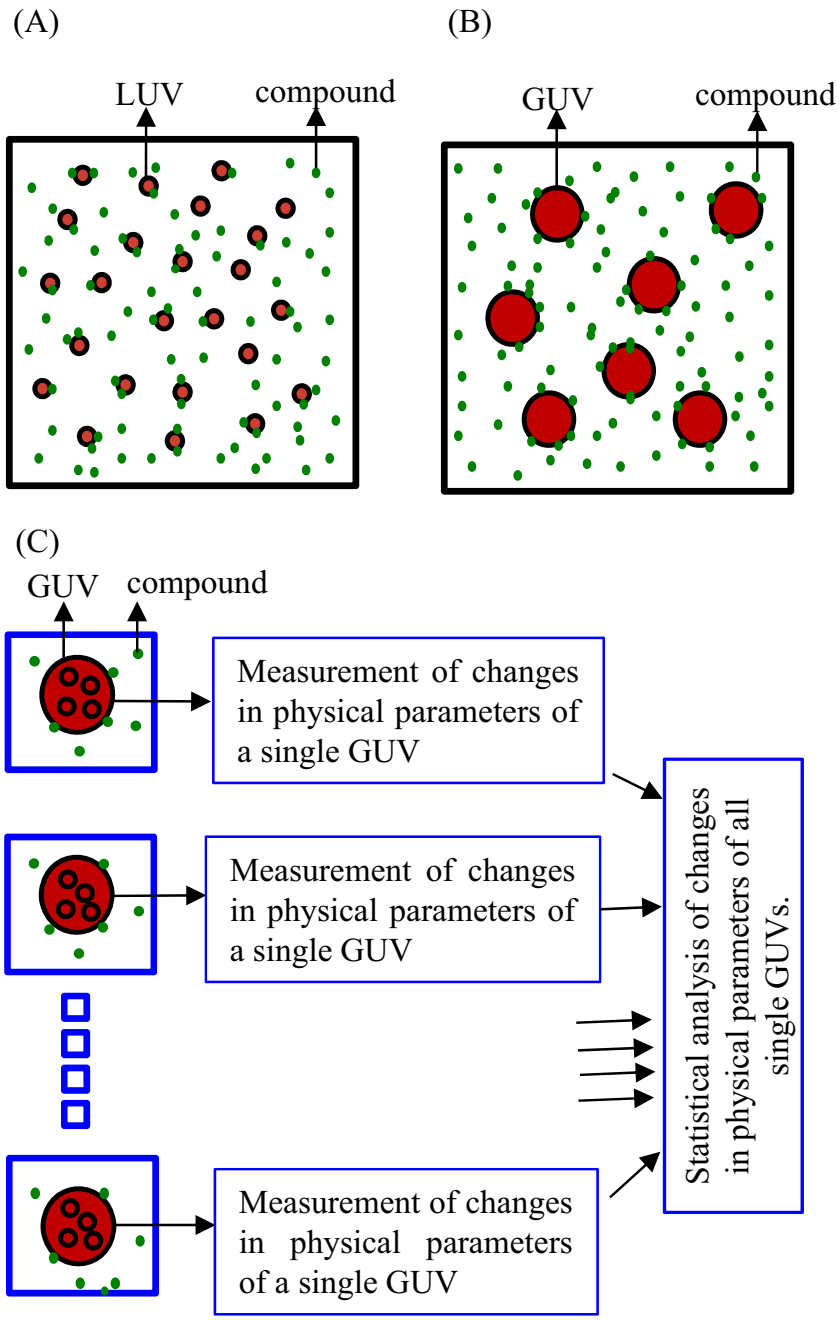

Fig. 1 Schemes of several experimental methods for entry of CPPs into lipid vesicles. **a** The LUV suspension method. In this method, compounds such as peptides are mixed with many LUVs in a suspension and then the ensemble averages of physical properties of all the LUVs in this suspension are measured using various biophysical and physicochemical techniques. The size of LUVs in this illustration is much larger than the real size (i.e., the real LUVs cannot be observed using optical microscopy), and the number of LUVs in this illustration is much smaller than the real number in most LUV suspensions. **b** The GUV suspension method. In this method, a compound solution is mixed with a suspension containing many GUVs, then the interaction of many GUVs in this suspension with compounds starts. The structures and physical properties of each GUV in this suspension during the interaction are measured using various types of optical microscopy. **c** The Single GUV method. In this method, a compound solution is continuously delivered to the vicinity of a single GUV through a micropipette during the interaction period under various types of optical microscopes. We continuously measure the changes in the structure and physical parameters of a single GUV that are induced by its interactions with the compound as a function of temporal and spatial coordinates using various types of optical microscopy

et al. 2013), and reduction of the fluorescent probe NBD attached to the CPP due to its reaction with dithionite (Terrone et al. 2003; Swiecicki et al. 2014). Early research indicated that CPPs could not enter LUV lumens although CPPs were able to enter GUV lumens (see details in the next sections) (Drin et al. 2001; Thorén et al. 2004). However, several recent reports indicate that CPPs can enter the lumen of LUVs with highly negatively charged membranes (Binder and Lindblom 2003; Walrant et al. 2013; Swiecicki et al. 2014).

Swiecicki et al. measured the internalization of NBD-labeled CPPs into LUVs comprising a mixture of dioleoylphosphatidylglycerol (DOPG) and dioleoylphosphatidylcholine (DOPC) (100 nm diameter) using the quenching of NBD fluorescence by reduction upon reaction with dithionite (Swiecicki et al. 2014). They found that some CPPs were internalized only if the LUVs contained a high mol fraction of DOPG (≥ 90 mol%). For example, 16% of NBD-R_9 and 9% of Tat (48–60) were internalized after 5-min reaction between 0.1 μM NBD-CPP with 10 μM DOPG-LUV. These authors also measured the CPP-induced transbilayer movement (i.e., flip-flop) of NBD-labeled phosphatidylglycerol (NBD-PG) in the outer monolayer using the quenching of NBD by dithionite. Several CPPs increased the rate of transbilayer diffusion of NBD-lipids, and the amount of NBD-PG transferred into the inner monolayer during interaction of the CPPs with the LUVs was proportional to the amount of CPP internalized. These authors speculated that these CPPs formed a neutral complex with negatively charged lipids in these inverted micelles and translocation of CPPs occurred through the formation of inverted micelles in the bilayer (see details later) (Swiecicki et al. 2014).

However, the LUV suspension method does not allow observation of CPP-induced structural changes in the LUVs. Generally, we can expect that large aggregations of LUVs occurs and membrane fusion between LUVs induces formation of multilamellar vesicles (MLVs) when highly negatively charged LUVs interact with highly positively charged CPPs through strong electrostatic attraction. The aggregation of the LUVs and the formation of the MLVs would suppress the reaction of dithionite with the NBD group of CPPs and PG, even if the NBD-CPPs and NBD-PG are located outside the LUVs. Therefore, without experimental data on the structure of LUVs after reaction with CPPs, it is difficult to judge the amount of internalized CPP and the amount of NBD-PG transferred into the inner monolayer.

The GUV suspension method

GUVs, or giant liposomes of lipid bilayers with diameters greater than 1 μm, have an advantage over LUVs because the shapes of GUVs, and physical quantities such as their fluorescence intensity in water or buffer, can be observed in real time with high spatial resolution using various forms of optical microscopy. Therefore, GUVs have been used for experiments to study shape changes, determination of the elastic modulus of lipid bilayers, phase separation, and tension-induced pore formation (Sandre et al. 1999; Rawicz et al. 2000; Baumgart et al. 2003; Tanaka et al. 2004).

Suspensions of many GUVs have been used (the GUV suspension method) to investigate the interaction of CPPs with vesicles (Fig. 1b). In this method, a compound solution is mixed with a suspension containing many GUVs, then the interaction of many GUVs in this suspension with compounds starts. The structures and physical properties of each GUV in this suspension during the interaction are measured using various types of optical microscopy. Using the GUV suspension method, Thorén et al. observed the entry of carboxyfluorescein (CF)-labeled penetratin (CF-penetratin) into GUVs of partially purified phosphatidylcholine (PC) membrane [PC/phosphatidylethanolamine (PE)/phosphatidylinositol (PI)/lyso-PC/cardiolipin (40/33/14/5/4)] in PBS buffer after 1 h interaction of CF-penetratin with GUVs at a high peptide/lipid molar ratio (1/46) (Thorén et al. 2000). They also found that the interaction of CF-penetratin with LUVs comprising the same lipids did not induce significant leakage of the internal contents. Similar investigations on the entry of CPPs into the GUV lumen were subsequently performed using the GUV suspension method (Thorén et al. 2004; Persson et al. 2004; Bárány-Wallje et al. 2005; Mishra et al. 2008; Ciobanasu et al. 2010; Mishra et al. 2011; Takechi et al. 2011; Walrant et al. 2013). For example, fluorescein isothiocyanate (FITC)-labeled R_6 (FITC-R_6) and rhodamine-labeled Tat (47–57) peptide separately induced substantial leakage of water-soluble fluorescent probes from the lumens of GUVs composed of dioleoylphosphatidylserine (DOPS) and dioleoyl-PE (DOPE), indicating that these peptides induced pore formation in DOPS/DOPE membranes, then these peptides entered the GUV lumen by diffusing through the pores (Mishra et al. 2008; Ciobanasu et al. 2010; Mishra et al. 2011). Mishra et al. demonstrated that the interaction of R_n with DOPS/DOPE (2/8) membranes induces the inverse bicontinuous double-diamond cubic phase (Q_{II}^D), leading the authors to propose that negative Gaussian curvature (i.e., saddle-splay) plays an important role in the entry of R_n and Tat into GUVs (Mishra et al. 2011). However, it is well known that inverse bicontinuous cubic phases, such as the Q_{II}^D phase, are formed only under special conditions dependent on lipid composition, temperature, water content, and salt concentration (Seddon and Templer 1995; Luzzati 1997; Aota-Nakano et al. 1999; Li et al. 2001; Okamoto et al. 2008; Oka et al. 2014). The formation of the cubic phase observed by Mishra et al. occurred due to the special lipid composition, i.e., DOPS and high concentrations of DOPE. In eukaryotic cells, DOPS is located only in the inner leaflet of the plasma membrane (Bigay and Antonny 2012), and hence CPPs interacting with the plasma membrane from the outside of the cell cannot interact with

DOPS in the inner leaflet. Therefore, DOPS cannot play an important role in the entry of CPPs into eukaryotic cells.

A new GUV suspension method was recently proposed (Wheaten et al. 2013), in which many GUVs containing smaller inner GUVs are suspended in a solution of a water-soluble fluorescent probe, carboxyfluorescein, and lissamine rhodamine B (Rh)-labeled CPPs (Rh-TP10W and Rh-DL1a). The authors observed that first carboxyfluorescein and the Rh-labeled peptides entered the inside of the outer GUV, and then the peptides translocated into the inside of the inner GUVs and there was an influx of carboxyfluorescein into the inner GUVs. Translocation of peptide into the inner GUVs occurred slowly (typically in 10 min) whereas the influx of carboxyfluorescein was rapid. However, using this method, it is difficult to obtain quantitative results, such as the peptide concentration dependence of peptide translocation and the rate constant of peptide-induced pore formation.

Some CPPs induce shape changes in GUVs. Qian et al. observed that FITC-labeled cyclic CPPs induced small budding on GUV membranes, which subsequently collapsed into aggregates composed of lipids and CPPs (Qian et al. 2016). These findings provide insights into the mechanism of entry of these CPPs into the cytosol of cells.

In most GUV suspension methods, the entry of CPPs into the GUV lumen is determined by comparing the fluorescence intensity (FI) of the inside of the GUVs with the FI outside the GUVs, but the sensitivity of this approach for detecting the entry of CPPs into the GUV lumen is rather low. If CPPs enter through pores, the FI of the inside of the GUVs greatly increases and it is easy to detect entry (e.g., Mishra et al. 2008; Ciobanasu et al. 2010; Mishra et al. 2011). However, if the efficiency of the entry of CPPs is low, it is difficult to detect entry using the GUV suspension method, especially at the beginning of the interaction. Moreover, in the GUV suspension method, we start to observe GUVs after mixing the peptide solution with the GUV suspension, making it difficult to observe the GUVs at the onset of the interaction of CPPs with GUVs.

The single GUV method

Characteristics of the methodology

The single GUV method was developed to investigate peptide/protein-induced leakage of the internal contents from vesicles following pore formation in lipid membranes or the rupture of vesicles (Tamba and Yamazaki 2005, 2009; Yamazaki 2008; Tamba et al. 2010; Alam et al. 2012; Islam et al. 2014b; Moniruzzaman et al. 2015). In this method, a compound solution is continuously delivered to the vicinity of a single GUV (with diameters greater than 10 μm) through a micropipette during the interaction period under various types of optical microscopes. We continuously measure the changes in the structure and physical parameters of a single GUV that are induced by its interactions with the compound as a function of temporal and spatial coordinates using fluorescence microscopy coupled with an electron multiplying charge-coupled device (EM-CCD) camera and confocal laser scanning microscopy (CLSM). The same experiment is repeated under identical conditions using many "single GUVs"; then, the results are analyzed statistically (Fig. 1c) (Yamazaki 2008). Thus, the single GUV method can reveal the details of elementary processes of individual events and allow determination of their kinetic constants. Using this method, various new data have been obtained on the elementary processes of pore formation (e.g., the rate constants both of pore formation and of membrane permeation (or leakage) through these pores) induced by antimicrobial peptides (AMPs) such as magainin 2 and lactoferricin B (LfcinB), and pore-forming toxins such as lysenin (Yamazaki 2008; Alam et al. 2012; Islam et al. 2014b; Moniruzzaman et al. 2015). It is possible to obtain the pore size and the time course of pore formation. For example, magainin 2 induced nanometer-sized pores that were large at the initial stage and then decreased to reach a steady, equilibrium size (Tamba et al. 2010). LfcinB induced local rupture, and hence, its pore size was large (Moniruzzaman et al. 2015). The antibacterial compound epigallocatechin gallate (EGCg) induced single GUV bursting, resulting in a globule composed of EGCg and lipids (Tamba et al. 2007).

A new method has been developed for studies of the interaction of CPPs with lipid bilayers by extending the single GUV method (Islam et al. 2014a). For this purpose, we prepare GUVs containing a water-soluble fluorescent probe such as AF647 and small GUVs 1–10 μm in diameter and examine the interaction of the fluorescent probe-labeled CPPs with these single GUVs using CLSM (Fig. 2). If the CPPs enter the GUV lumen, they bind to the membrane of the small GUVs inside the mother GUV, resulting in fluorescence. Therefore, by observing the fluorescent, small GUVs in the mother GUV, we can detect the entry of CPPs into the lumen of the mother GUV. One merit of this method is the highly sensitive detection of CPPs due to both the large binding constants of CPPs to membranes (i.e., the CPPs are concentrated in the membrane) and the larger quantum efficiency of the fluorescence of fluorescent probes in the membrane compared to in aqueous solution (Lakowicz 2006).

Moreover, using the single GUV method, we can observe single GUVs and measure the physical properties of each GUV from the start ($t = 0$) of the interaction with compounds, which is a major advantage over the GUV suspension method (Yamazaki 2008; Islam et al. 2014b). We can therefore observe the initial entry of CPPs into the GUV lumen from between 0 to 10 min after the interaction of CPPs with single GUVs, whereas in most GUV suspension method experiments the entry of CPPs is observed after 1 h of interaction. Another merit of the single GUV method is in obtaining the relationship between the entry of CPPs into the GUV lumen and the leakage of a water-

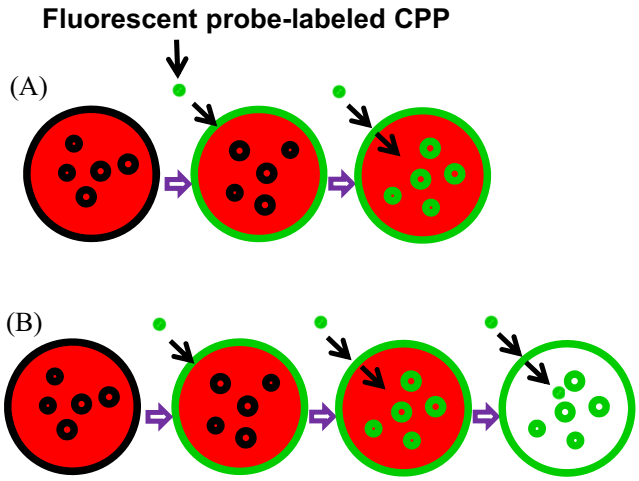

Fig. 2 A schematic drawing of the detection of entry of CPPs into the GUV lumen using single GUVs containing small GUVs. **a** Entry of CPPs into the GUV lumen without leakage of a water-soluble fluorescent probe (i.e., no pore formation in the GUV membrane). **b** Entry of CPPs into the GUV lumen before pore formation and subsequent leakage of a water-soluble fluorescent probe (i.e., pore formation in the GUV membrane). Red color in the GUV lumen indicates the FI due to a water-soluble fluorescent probe such as AF647, and green color indicates the FI due to fluorescent probe-labeled CPPs such as CF-TP10 and CF-R_9

soluble fluorescent probe such as AF647 (i.e., pore formation in the GUV membrane). In the single GUV method, we can detect pore formation from the beginning of the interaction, greatly facilitating the determination of this relationship.

In the single GUV method, a peptide solution is continuously delivered to the vicinity of a single GUV through a micropipette during the interaction period, allowing the peptide concentration in the vicinity of a single GUV to be kept at approximately the concentration inside the micropipette (Karal et al. 2015). In contrast, in suspension methods using GUVs (or LUVs), many GUVs (or LUVs) are added to a given concentration of peptide solution, and hence, the peptide concentration outside the GUVs (or LUVs) depends on the GUV (or LUV) concentration (i.e., lipid concentration) of the suspension. This concentration cannot be controlled well, and it changes with time because the binding of peptides with the GUV (or LUV) membranes and the entry of peptides into the lumen of the GUVs (or LUVs) both increase with time.

In the following sections, we summarize detailed information obtained using the single GUV method with GUVs containing small GUVs.

Relationship between the entry of CPPs into the GUV lumen and CPP-induced pore formation

We studied the interaction of CF-labeled TP10 (CF-TP10) with DOPG/DOPC (2/8; molar ratio)-GUVs at high peptide concentrations (≥ 1.9 μM) in aqueous solution outside the GUVs. We observed that first CF-TP10 entered the GUV lumen, and then pores formed subsequently. For example, Fig. 3 shows the interaction of 1.9 μM CF-TP10 with DOPG/DOPC (2/8)-GUVs. The FI of the GUV lumen due to the water-soluble fluorescent probe AF647 was constant until 210 s, then rapidly decreased (Fig. 3 (1)), indicating that pore formation was initiated at 210 s and then AF647 leaked through the pores (i.e., the diffusion of AF647 from the GUV lumen to the outside of the GUV occurred through the pores). On the other hand, the FI of the GUV membrane (i.e., the rim intensity) due to CF-TP10 increased rapidly after initiation of the interaction at $t = 0$; then, fluorescence was observed in the small vesicles in the GUV lumen after 140 s (Fig. 3 (2)). These results indicate that first the CF-TP10 concentration in the GUV membrane rapidly increased and then CF-TP10 entered the GUV lumen to bind to the small vesicles. Consequently, the translocation of CF-TP10 across the GUV membrane and subsequent entry of CF-TP10 into the GUV lumen occurred before pore formation. Figure 2b schematically shows this mode of entry of CPPs into the GUV lumen (i.e., the entry of CPPs into the GUV lumen occurs before pore formation, and then pore formation occurs). Using the single GUV method, we can obtain the rate constant of peptide/protein-induced pore formation and also the size of the pores (Tamba and Yamazaki 2005, 2009; Tamba et al. 2010; Alam et al. 2012; Moniruzzaman et al. 2015), as demonstrated using CF-TP10 (or TP10) (Islam et al. 2014a).

On the other hand, at lower peptide concentrations (from 0.6 to 1.0 μM) than those used in the above experiments, CF-TP10 entered the lumen of DOPG/DOPC (2/8)-GUVs after a lag time from the increase in rim intensity, while the FI of the GUV lumen due to AF647 was constant up to 6 min, showing that no leakage of AF647 occurred. These results indicate that CF-TP10 entered the lumen without pore formation during the initial 6-min interaction (Islam et al. 2014a). Figure 2a schematically shows this mode of entry of CPPs into GUV lumens (i.e., the entry of CPPs without pore formation). The entry of CF-labeled R_9 (CF-R_9) into GUVs with most lipid compositions during initial 6-min interaction (Sharmin et al. 2016), and the entry of rhodamine-labeled lactoferricin B (4–9) (Rh-LfcinB (4–9); RRWQWR) into DOPG/DOPC (5/5)-GUVs during initial 10-min interaction (Moniruzzaman et al. 2017), use this mode of entry (Fig. 2a).

In the interaction of high concentrations of CF-labeled R_9 (CF-R_9) with GUVs composed of dilauroyl-PG (DLPG)/ditridecanoyl-PC (DTPC) (4/6), CF-R_9 induced pore formation in the lipid bilayer and then entered the GUV lumen through the pores (Fig. 4). The entry of peptides through the pores was much more efficient compared to entry without pore formation: the CF-R_9 concentration in the lumen of DLPG/DTPC (4/6)-GUVs at 6 min was almost the same as that outside the GUVs (i.e., 100% entry), whereas the CF-R_9 concentration in the lumen of DOPG/DOPC (2/8)-GUVs at 6 min (where entry occurred without pore formation) was less than 1% of that in the outside solution (Sharmin et al. 2016).

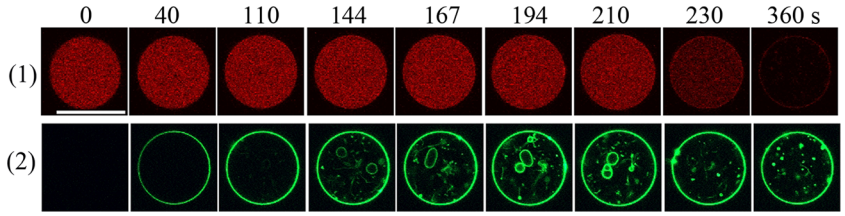

Fig. 3 Entry of CF-TP10 into a single GUV and subsequent CF-TP10-induced pore formation. The single DOPG/DOPC (2/8)-GUV containing small GUVs was interacted with 1.9 μM CF-TP10. CLSM images of (1) AF647 and (2) CF-TP10. The numbers above each image show the time in seconds after CF-TP10 addition was started. The bar corresponds to 30 μm. This figure is cited from the ref. of Islam et al. (2014a) with a permission of American Chemical Society

Rate of entry of CPPs into the lumen of single GUVs

In the current single GUV method for CPPs, the entry of CPPs is determined from the presence of visible, small fluorescent vesicles in the GUV lumen. Thus, the fraction of GUVs containing fluorescent small vesicles in their lumen at a specific time t among all the examined GUVs, P_{entry} (t), is used as a measure of the rate of entry of CPPs into the GUV lumen (Islam et al. 2014a). P_{entry} (t) was found to increase with time and with an increase in CPP concentration (Islam et al. 2014a; Sharmin et al. 2016; Moniruzzaman et al. 2017), and P_{entry} (6 min) of CF-R_9 greatly depended on the lipid composition of the GUV. First, P_{entry} (6 min) increased with DOPG concentration in the DOPG/DOPC membrane (indicating that the rate of entry increased with an increase in electrostatic interactions) (Sharmin et al. 2016). Second, P_{entry} (6 min) of CF-R_9 into DLPG/DTPC (2/8) GUVs was larger than that into DOPG/DOPC (2/8) GUVs, and P_{entry} (6 min) was 0 for DOPG/DOPC membranes containing a high concentration of cholesterol (DOPG/DOPC/chol (2/6/4)), indicating that the line tension (i.e., free energy of the edge of the prepore per unit length) of the prepore rim in lipid bilayers greatly affected the rate of entry of CF-R_9 (Sharmin et al. 2016). A high concentration of cholesterol also inhibited the entry of CF-TP10 into DOPG/DOPC/chol (2/6/4)-GUVs when the concentration of CF-TP10 was low (≤ 1.0 μM) (although the rate of entry of 1.0 μM CF-TP10 into DOPG/DOPC (2/8)-GUV was large) (Islam et al. 2017). However, higher concentrations of CF-TP10 induced pore formation in the same DOPG/DOPC/chol (2/6/4)-GUV membrane and CF-TP10 subsequently entered the GUV lumen through the pore. Hence, the rate of entry of CF-TP10 into DOPG/DOPC/chol (2/6/4)-GUV increased with CF-TP10 concentration above 2.0 μM because the rate of pore formation increased (Islam et al. 2017).

Analysis of the rim intensity of single GUVs and rate constants of binding/unbinding of CPPs to/from membranes

We can obtain the time course of the FI of membranes of single GUVs (i.e., rim intensity) due to fluorescent probe-labeled CPPs from the start of the interaction of the CPPs with the single GUVs. When the rim intensity is proportional to the CPP concentration in the GUV membrane, we can convert the time course of the rim intensity into that of the CPP concentration in the membrane. Fitting the time course of rim intensity to the theoretical equation of the CPP concentration in the GUV membranes, C_M, as follows provides an apparent rate constant for the increase in rim intensity, k_{app} (Islam et al. 2014a):

$$C_M(t) = A\left[1-\exp\left(-k_{app}t\right)\right] \quad (1)$$

$$\text{where } k_{app} = k_{ON}C_{out}^{eq}/2 + k_{OFF} \quad (2)$$

where k_{ON} is the rate constant of the binding of CPPs to the GUV monolayer, and k_{OFF} is the rate constant of unbinding of the CPPs from the monolayer to the

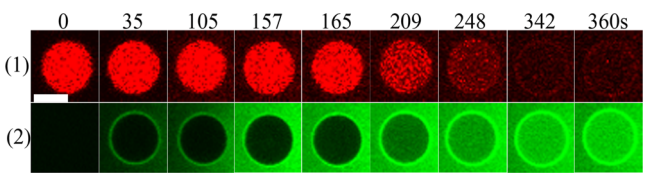

Fig. 4 CF-R_9-induced pore formation in a GUV membrane and subsequent entry of CF-R_9 into a single GUV. The single DLPG/DTPC (4/6)-GUVs not containing small vesicles was interacted with 40 μM CF-R_9. CLSM images of (1) AF647 and (2) CF-R_9. The numbers above each image show the time in seconds after the addition of CF-R_9 was started. The bar corresponds to 10 μm. This figure is cited from the ref. of Sharmin et al. (2016) with a permission of American Chemical Society

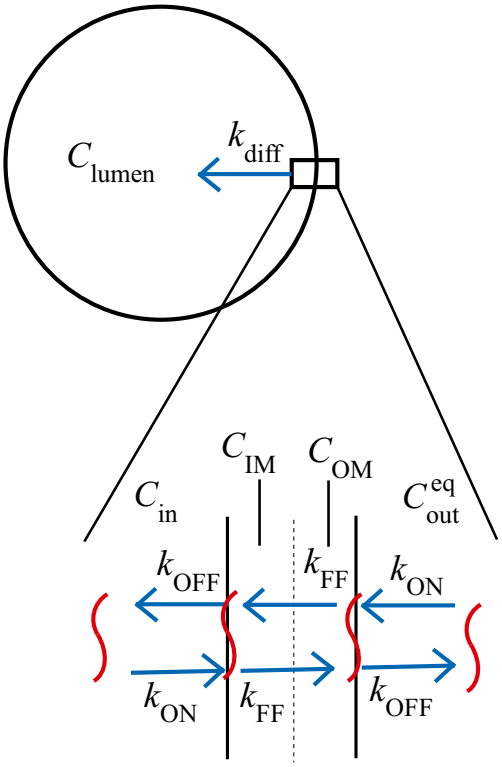

Fig. 5 A scheme of the elementary processes of entry of CPPs into single GUVs. C_{lumen}, C_{in}, and C^{eq}_{out} are CPP concentration in the GUV bulk lumen, in the GUV lumen adjacent to the membrane, and in aqueous solution outside the GUV adjacent to the membrane. C_{OM} and C_{IM} are CPP concentration in the outer and inner leaflet of the GUV, respectively. k_{ON}, k_{OFF}, and k_{diff} are rate constant of the binding of CPPs to the leaflet of a GUV from aqueous solution, of unbinding of CPPs from the leaflet to the aqueous solution adjacent to the membrane, and of the diffusion from the GUV lumen adjacent to the membrane to the bulk lumen (i.e., the central region of the GUV). k_{FF} is the rate constant of the translocation of CPPs from one leaflet to the other. This figure is cited from the ref. of Sharmin et al. (2016) with a permission of American Chemical Society

aqueous solution (Fig. 5). Thus, the binding constant of CPPs to the membrane, K_B, is $K_B = k_{ON}/k_{OFF}$. The dependence of k_{app} on the CPP concentration in aqueous solution, $C_{out}{}^{eq}$, provides the values of k_{ON} and k_{OFF} according to Eq. 2 (Islam et al. 2014a; Sharmin et al. 2016; Moniruzzaman et al. 2017). These rate constants greatly depend on the lipid composition (Sharmin et al. 2016).

The saturated, steady rim intensity provides different information. In the interaction of CF-R_9 and CF-TP10 with single GUVs, high concentrations of cholesterol in the GUV membrane decreased the saturated rim intensity to half that in the absence of cholesterol, indicating that cholesterol greatly suppressed the translocation of CF-R_9 and CF-TP10 from the outer leaflet to the inner leaflet (Sharmin et al. 2016; Islam et al. 2017). This is the main reason why these CPPs do not enter the lumens of GUVs containing a high concentration of cholesterol.

Effect of membrane tension on the entry of CPPs into the GUV lumen

In the single GUV method, we can control the mechanical state of the membranes of single GUVs during the interaction of peptides/proteins by applying the membrane tension of each GUV, and hence, we can examine the effects of membrane tension on the interaction of peptides/proteins with a GUV membrane. The membrane tension of a single GUV can be controlled using the micropipette aspiration method (Rawictz et al. 2000), whereby producing a pressure difference between the inside and the outside of a GUV applies mechanical tension on the GUV membrane. This method has allowed the investigation of tension-induced rupture of GUVs (Evans et al. 2003; Evans and Smith 2011; Levadny et al. 2013; Karal et al. 2016) and the effects of membrane tension on AMP-induced pore formation (Karal et al. 2015).

Islam et al. examined the effect of mechanical tension on the rate of entry of CF-TP10 into DOPG/DOPC (2/8)-GUVs: P_{entry} (6 min) increased with an increase in membrane tension, and the rate constants (k_{ON} and k_{OFF}) also depended on membrane tension (Islam et al. 2017).

Single GUVs containing LUVs vs. single GUVs containing small GUVs

Above, we summarized the results obtained using the single GUV method with GUVs containing small GUVs. However, this method cannot provide quantitative information on the time course of the amount of fluorescent probe-labeled CPP entering into the GUV lumen because the number of small GUVs inside the GUV lumen is limited and the small GUVs move rapidly due to Brownian motion. Consequently, the FI due to small GUVs in the focal plane of the CLSM fluctuates with time. Moreover, the number and size of small GUVs in the GUV lumen greatly depend on the GUVs. Some GUVs have relatively large GUVs (greater than 10 μm in diameter) in their lumens (e.g., Fig. 3), but other GUVs have only small GUVs (less than 10 μm). Very recently, a new single GUV method using GUVs containing LUVs has been developed (Moghal et al. 2018). This method can continuously detect the entry of CF-TP10 into single GUVs and follow the time course of CF-TP10 concentration in the GUV lumen continuously and quantitatively. This is therefore a promising method for monitoring the time course of entry of CPPs into single GUVs.

Pathways of the translocation of CPPs across lipid bilayers and the mechanism of translocation

The above results on the interaction of CPPs with lipid vesicles clearly indicate that CPPs can translocate across lipid

bilayers, indicating that in principle special proteins and other mechanisms in cells are not required for the entry of CPPs into the cytosol of cells. Several models for the mechanisms and pathways for the translocation of CPPs across lipid bilayers have been proposed. Here, we describe three models.

Model A: translocation of CPPs through pores

In model A, CPPs can induce the formation of pores through which water-soluble fluorescent probes leak out from the vesicles, and subsequently, the CPPs permeate through the pores to enter the vesicle lumen (Fig. 6a) (Mishra et al. 2008; Ciobanasu et al. 2010; Mishra et al. 2011). Here, we define a pore as a water channel in a lipid membrane that is always open and whose diameter is sufficiently large so that fluorescent probes such as AF647 can pass through the pore. It is believed that the entry of Tat into DOPS/DOPE-GUVs (Mishra et al. 2008) and of oligoarginine into DOPS/DOPE-GUVs (Mishra et al. 2011) and DLPG/DTPC (4/6)-GUVs (Sharmin et al. 2016) follow model A. However, in this model, any peptides/proteins inducing large pores through which these peptides enter vesicles and cells can be considered as CPPs in a wider sense. For example, magainin 2, an AMP, enters single vesicles through pores that it induces (Karal et al. 2015).

Model B: translocation of CPPs through transient prepores

In model B, the translocation of CPPs occurs through transient hydrophilic prepores in the membrane (Fig. 6b) (Sharmin et al. 2016; Islam et al. 2017). In this model, water-soluble fluorescent probes cannot leak out from the vesicles (Fig. 2a). It is believed that the entry of TP10 into DOPG/DOPC (2/8)-GUVs (Islam et al. 2014a), the entry of oligoarginine (R_9) into DOPG/DOPC-GUVs and DLPG/DTPC (2/8)-GUVs (Sharmin et al. 2016), and the entry of Rh-LfcinB (4–9) into DOPG/DOPC (5/5)-GUVs (Moniruzzaman et al. 2015), all follow model B. The thermal fluctuations of lipid bilayers in the liquid-crystalline phase are large, resulting in fluctuation of their local lateral density, such as rarefaction (i.e., an area of decreased density of lipids) called a prepore (Fig. 7) (Evans et al. 2003; Evans and Smith 2011; Levadny et al. 2013; Karal et al. 2016; Akimov et al. 2017). Such prepores are unstable due to the large line tension, Γ, at the edges of prepores, and hence, they immediately close (Glaser et al. 1988; Fuertes et al. 2011). However, if the membrane tension is increased due to external forces and stretching of the membrane, pore formation occurs through which internal contents leak to the outside of the vesicles because the membrane tension greatly decreases the activation energy of pore formation (Evans et al. 2003; Evans and Smith 2011; Levadny et al. 2013; Karal et al. 2016; Akimov et al. 2017). The interaction of CPPs with these prepores may stabilize the prepores by decreasing their line tension. A prepore is believed to have a toroidal-like structure (Fig. 6b) similar to the structure of a pore (Fig. 6a): two monolayers bend and connect with each other at the wall of the

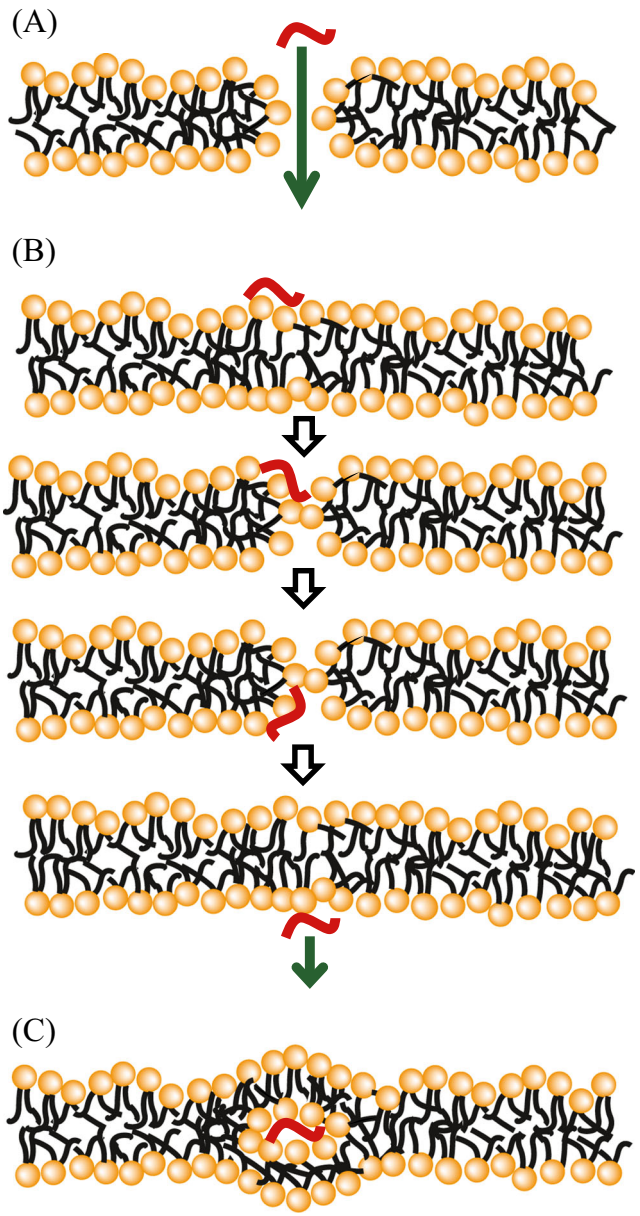

Fig. 6 A schematic drawing of three models for the pathway of translocation of CPPs across lipid bilayers. **a** Translocation of CPPs through pores in lipid bilayers. A pore is defined as a water channel in a lipid membrane that is always open and whose diameter is sufficiently large so that fluorescent probes such as AF647 can pass through the pore. **b** Translocation of CPPs through transient prepores in lipid bilayers. CPP molecules bound to negatively charged lipids in the outer leaflet can diffuse laterally in the connected monolayers at the wall of a toroidal prepore, then diffuse into the inner leaflet (i.e., the translocation of CPPs via lateral diffusion). **c** Translocation of CPPs via inverted micelle formation in lipid bilayers. In inverted micelles, positively charged CPPs form a neutral complex with negatively charged lipids, which can translocate across the bilayer. There is a defined stoichiometry of CPPs and charged lipids during transfer

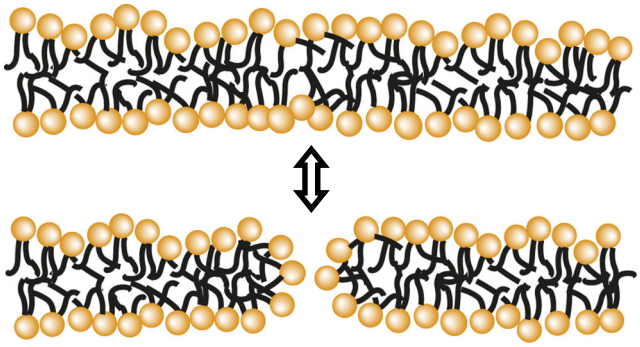

Fig. 7 A schematic drawing of a prepore in a lipid bilayer. Thermal fluctuations of lipid bilayers in the liquid-crystalline phase are large, resulting in fluctuation of their local lateral density such as rarefaction (i.e., an area of decreased density of lipids) called a prepore. Such prepores are unstable due to large line tension at the edge of prepores, and hence immediately close

toroidal pore (Evans et al. 2003; Karal et al. 2016). Therefore, CPP molecules bound to negatively charged lipids in the outer leaflet can diffuse laterally in the connected monolayers at the wall of a toroidal prepore, then diffuse into the inner leaflet (i.e., the translocation of CPPs via lateral diffusion). This induces the transfer of negatively charged lipids from the outer leaflet to the inner leaflet concomitant with the transfer of CPP molecules, which may explain the observed co-internalization of CPPs and negatively charged lipids (Swiecicki et al. 2014). The line tension Γ depends on the lipid composition: Γ of DLPG/DTPC is smaller than Γ of DOPG/DOPC, which makes the prepores more stable, and thus, the frequency of prepore formation and the size of prepores in DLPG/DTPC are larger than those of DOPG/DOPC (Sharmin et al. 2016). Similarly, Γ of DOPG/DOPC/chol (2/6/4) is larger than Γ of DOPG/DOPC (2/8) due to the effect of a high concentration of cholesterol (Karatekin et al. 2003). Cholesterol destabilizes the prepores, and thus, the frequency of prepore formation and the size of prepores in DOPG/DOPC/chol (2/6/4) are smaller than those of DOPG/DOPC. These values of Γ can reasonably explain the result of the rate of entry of CF-R_9 into single GUVs (Sharmin et al. 2016). The application of membrane tension by an external force increases the stability of prepores (Evans et al. 2003; Levadny et al. 2013), and thus, the frequency of prepore formation and the size of prepores increases with tension, consistent with the effect of membrane tension on the rate of entry of CF-TP10 into single GUVs (Islam et al. 2017).

Model C: translocation of CPPs via inverted micelle formation

In model C, the translocation of CPPs occurs via inverted micelle formation (Fig. 6c) (Berlose et al. 1996; Swiecicki et al. 2014). In inverted micelles, positively charged CPPs form a neutral complex with negatively charged lipids, which can translocate across the bilayer. There is a defined stoichiometry of CPPs and charged lipids during transfer. It is believed that the entry of Tat and oligoarginine into vesicles composed of highly negatively charged membranes (the mol fraction of negatively charged lipid is larger than 0.90) (Swiecicki et al. 2014) follow model C.

Molecular dynamics simulation of the translocation of CPPs across lipid bilayers

Studies of the translocation of CPPs across lipid bilayers using molecular dynamics (MD) simulation have recently increased (Herce and Garcia 2007; Yesylevskyy et al. 2009; Herce et al. 2009; Kawamoto et al. 2011; Sun et al. 2014, 2015). As described above, the single GUV method provides experimental data regarding the time course of the entry of CPPs, the concentration of CPPs in the membrane, and the leakage of fluorescent probes from the initial time of the interaction, and thus, it is possible to quantitatively compare these experimental results with those obtained using MD simulation. At the present stage of all-atom MD simulation, the time and the area of membrane that can be simulated are very limited and thus prepore formation cannot be observed in MD simulations of lipid bilayers, although tension-induced pore formation has been investigated (Wohlert et al. 2006). Progress in MD simulation in the near future could provide new information on the translocation of CPPs across bilayers.

Interaction of CPPs with bacterial cells

Studies on the interaction of CPPs with lipid vesicles provide fundamental information on the translocation of CPPs across lipid bilayers and the entry of CPPs into lipid vesicles. This information is very helpful in elucidating the mechanism of entry of CPPs into the cytosol of eukaryotic cells via not only direct translocation across the plasma membrane, but also by endocytosis. In eukaryotic cells, there may be more factors involved in the translocation of CPPs across the plasma membrane compared to their translocation across vesicle membranes, but it is important to keep in mind that CPPs themselves can pass through lipid bilayers unaided due to their strong interactions with the membrane.

Most prokaryotic cells such as bacteria typically have a simple membrane system (e.g., no endocytosis (Lonhienne et al. 2010) and no membrane vesicles in the cytoplasm). Therefore, bacterial cells may be useful for elucidating the mechanism of entry of CPPs into the cytosol. The interactions of CPPs such as TP10, penetratin, and pVEC with bacterial cells such as *Escherichia coli* have been investigated using a suspension of bacterial cells and the results indicate that these

peptides have antimicrobial activities (Palm et al. 2006; Nekhotiaeva et al. 2004). TP10 and pVEC entered eukaryotic cells without affecting viability but killed bacterial cells preferentially. The interaction of these CPPs with bacterial cells induced the rapid entry of SYTOX green into their cytoplasm, indicating that CPPs damaged the plasma membrane, increasing its permeability (Nekhotiaeva et al. 2004). The amounts of penetratin and pVEC entering into bacterial cells were estimated using fluorescence HPLC (Palm et al. 2006).

Recently, the interaction of Rh-LfcinB (4–9) with single cells of *E. coli* (JM-109) containing calcein in their cytoplasm was investigated using CLSM by a method similar to the single GUV method (Fig. 1c) (Moniruzzaman et al. 2017). The minimum inhibitory concentrations (MICs) of Rh-LfcinB (4–9) and LfcinB (4–9) against *E. coli* were 5 ± 1 and 25 ± 10 μM, respectively, and the hemolytic activities of these peptides were low. Rh-LfcinB (4–9) entered the cytoplasm of single cells of *E. coli* without leakage of calcein. SYTOX green did not enter *E. coli* cells when Rh-LfcinB (4–9) and LfcinB (4–9) interacted with the cells in a suspension. These results indicate that Rh-LfcinB (4–9) and LfcinB (4–9) did not induce damage of the *E. coli* plasma membrane, and hence, damage to the membrane is not the main cause of the antimicrobial activities of these peptides. Strong interactions of Rh-LfcinB (4–9) and LfcinB (4–9) with DNA molecules were observed, suggesting that antimicrobial activity might be due to binding of the peptides with DNA (Moniruzzaman et al. 2017). It is noted that the results of the interaction of Rh-LfcinB (4–9) with lipid vesicles obtained using the single GUV method are consistent with the interaction of this peptide with *E. coli* cells.

Concluding remarks

In this mini-review, we summarized our current knowledge of the entry of CPPs into lipid bilayer vesicles and bacterial cells. CPPs can translocate across lipid bilayers and enter vesicles, but the efficiency of entry of a CPP greatly depends on the lipid composition and the type of CPP. We described three models for the pathways of translocation of CPPs across lipid bilayers, but the mechanisms underlying these pathways remain poorly understood and require further studies using new experiments, simulations, and theories. The single GUV method provides detailed information on the elementary processes of the entry of CPPs into vesicles, which is helpful in elucidating the mechanisms of entry. Our evolving understanding of the mechanisms underlying the translocation of CPPs across lipid bilayers and their entry into lipid vesicles has led us to reconsider the mechanisms by which CPPs enter the cytosol of various eukaryotic cells. Early studies on CPPs suggested that endocytosis is the main pathway of entry of CPPs into eukaryotic cells, but recent experimental data increasingly support the direct translocation of CPPs across the plasma membrane (Ter-Avetisyan et al. 2009; Wang et al. 2016). Moreover, the entry of CPPs into bacterial cells without damaging the plasma membrane (Moniruzzaman et al. 2017) supported direct translocation across plasma membranes because most bacterial cells do not have endocytosis systems (Lonhienne et al. 2010). Other factors (such as special proteins/peptides and lipids) in the plasma membrane of eukaryotic cells may affect the rate and the pathways of entry of CPPs into the cytosol. However, the effects of these factors on the entry of CPPs are additional to the fundamental characteristics of the translocation of CPPs across lipid bilayers and the entry of CPPs into lipid vesicles.

Funding This work was supported in part by a Grant-in-Aid for Scientific Research (B) (No. 15H04361) from the Japan Society for the Promotion of Science (JSPS) to M.Y. This work was also supported in part by the Cooperative Research Project of the Research Center for Biomedical Engineering.

Compliance with ethical standards

Ethical approval This article does not contain any studies with human participants or animals performed by any of the authors.

Conflict of interest The authors declare that they have no conflict of interest.

References

Akimov SA, Volynsky PE, Galimzyanov TR, Kuzmin PI, Pavlov KV, Batishchev OV (2017) Pore formation in lipid membrane I: continuous reversible trajectory from intact bilayer through hydrophobic defect to transversal pore. Sci Rep 7:12152

Alam JM, Kobayashi T, Yamazaki M (2012) The single giant unilamellar vesicle method reveals lysenin-induced pore formation in lipid membranes containing sphingomyelin. Biochemistry 51:5160–5172

Aota-Nakano Y, Li SJ, Yamazaki M (1999) Effects of electrostatic interaction on the phase stability and structures of cubic phases of monoolein/oleic acid mixture membranes. Biochim Biophys Acta 1461:96–102

Bárány-Wallje E, Keller S, Serowy S, Geibel S, Pohl P, Bienert M, Dathe M (2005) A critical reassessment of penetratin translocation across lipid membranes. Biophys J 89:2513–2521

Bárány-Wallje E, Gaur J, Lundberg P, Langle Ű, Gräslund A (2007) Differential membrane perturbation caused by the cell penetrating peptide TP10 depending on attached cargo. FEBS Lett 581:2389–2393

Baumgart T, Hess ST, Webb WW (2003) Imaging coexisting fluid domains in biomembrane models coupling curvature and line tension. Nature 425:821–824

Bechara C, Sagan S (2013) Cell-penetrating peptides: 20 years later, where do we stand? FEBS Lett 587:1693–1702

Berlose J-P, Convert O, Derossi D, Brunissen A, Chassaing G (1996) Conformational and associative behaviours of the third helix of antennapedia homeodomain in membrane-mimetic environments. Eur J Biochem 242:372–386

Bigay J, Antonny B (2012) Curvature, lipid packing, and electrostatics of membrane organelles: defining cellular territories in determining specificity. Dev Cell 23:886–895

Binder H, Lindblom G (2003) Charge-dependent translocation of the trojan peptide penetratin across lipid membranes. Biophys J 85: 982–995

Ciobanasu C, Siebrasse J, Kubitscheck U (2010) Cell-penetrating HIV1 TAT peptides can generate pores in model membranes. Biophys J 99:153–162

Doherty GJ, McMahon HT (2009) Mechanisms of endocytosis. Annu Rev Biochem 78:857–902

Drin G, Déméné H, Temsamani J, Brasseur R (2001) Translocation of the pAntp peptide and its amphipathic analogue AP-2AL. Biochemistry 40:1824–1834

Duchardt F, Fotin-Mieczek M, Schwarz H, Fischer R, Brock R (2007) A comprehensive model for the cellular uptake of cationic cell-penetrating peptides. Traffic 8:848–866

EL-Andaloussi S, Johansson H, Magnusdottir A, Järver P, Lundberg P, Langel Ű (2005) TP10, a delivery vector for decoy oligonucleotides targeting the Myc protein. J Control Release 110:189–201

Elmquist A, Lindgren M, Bartfai T, Langel U (2001) VE-cadherin-derived cell-penetrating peptide, VEC, with carrier functions. Exp Cell Res 269:237–244

El-Sayed A, Futaki S, Harashima H (2009) Delivery of macromolecules using arginine-rich cell-penetrating peptides: ways to overcome endosomal entrapment. AAPS J 11:13–21

Evans E, Smith BA (2011) Kinetics of hole nucleation in biomembrane rupture. New J Phys 13:095010

Evans E, Heinrich V, Ludwig F, Rawicz W (2003) Dynamic tension spectroscopy and strength of biomembranes. Biophys J 85:2342–2350

Fischer R, Köhler K, Fotin-Mleczek M, Brock R (2004) A stepwise dissection of the intracellular fate of cationic cell-penetrating peptides. J Biol Chem 279:12625–12635

Fuertes G, Giménez D, Esteban-Martín S, Sánchez-Muñoz O, Salgado J (2011) A lipocentric view of peptide-i nduced pores. Eur Biophys J 40:399–415

Futaki S, Suzuki T, Ohashi W, Yagami T, Tanaka S, Ueda K, Sugiura Y (2001) Arginine-rich peptides. An abundant source of membrane-permeable peptides having potential as carriers for intracellular protein delivery. J Biol Chem 276:5836–5840

Glaser RW, Leikin SL, Chernomordik LV, Pastushenko VF, Sokirko AI (1988) Reversible electrical breakdown of lipid bilayers: formation and evolution of pores. Biochim Biophys Acta 940:275–287

Herce HD, Garcia AE (2007) Molecular dynamics simulations suggest a mechanism for translocation of the HIV-1 TAT peptide across lipid membranes. Proc Natl Acad Sci U S A 104:20805–20810

Herce HD, Garcia AE, Litt J, Kane RS, Martin P, Enrique N, Rebolledo A, Milesi V (2009) Arginine-rich peptides destabilizes the plasma membrane, consistent with a pore formation translocation mechanism of cell-penetrating peptides. Biophys J 97:1917–1925

Hille B (1992) Ionic channels of excitable membranes, 2nd edn. Sinauer Association Inc., Massachusetts

Islam MZ, Ariyama H, Alam JM, Yamazaki M (2014a) Entry of cell-penetrating peptide transportan 10 into a single vesicle by translocating across lipid membrane and its induced pores. Biochemistry 53:386–396

Islam MZ, Alam JM, Tamba Y, Karal MAS, Yamazaki M (2014b) The single GUV method for revealing the functions of antimicrobial, pore-forming toxin, and cell-penetrating peptides or proteins. Phys Chem Chem Phys 16:15752–15767

Islam MZ, Sharmin S, Levadnyy V, Shibly SUA, Yamazaki M (2017) Effects of mechanical properties of lipid bilayers on entry of cell-penetrating peptides into single vesicles. Langmuir 33:2433–2443

Karal MAS, Alam JM, Takahashi T, Levadny V, Yamazaki M (2015) Stretch-activated pore of antimicrobial peptide Magainin 2. Langmuir 31:3391–3401

Karal MAS, Levadnyy V, Yamazaki M (2016) Analysis of constant tension-induced rupture of lipid membranes using activation energy. Phys Chem Chem Phys 18:13487–13495

Karatekin E, Sandre O, Guitouni H, Borghi N, Puech P–H, Brochard-Wyart F (2003) Cascades of transient pores in giant vesicles: line tension and transport. Biophys J 84:1734–1749

Kawamoto S, Takasu M, Miyakawa T, Morikawa R, Oda T, Futaki S, Nagao H (2011) Inverted micelles formation of cell-penetrating peptide studied by coarse-grained simulation: importance of attractive force between cell-penetrating peptides and lipid head group. J Chem Phys 134:095103

Ladokhin AS, Wimley WC, White SH (1995) Leakage of membrane vesicle contents: determination of mechanism using fluorescence requenching. Biophys J 69:1964–1971

Lakowicz JR (2006) Principles of fluorescence spectroscopy, 3rd edn. Springer, New York

Levadny V, Tsuboi T, Belaya M, Yamazaki M (2013) Rate constant of tension-induced pore formation in lipid membranes. Langmuir 29: 3848–3852

Li SJ, Yamashita Y, Yamazaki M (2001) Effect of electrostatic interactions on phase stability of cubic phases of membranes of monoolein/dioleoylphosphatidic acid mixture. Biophys J 81:983–993

Lipowsky R, Sackmann E (eds) (1995) Structure and dynamics of membranes. Elsevier Science BV, Amsterdam

Lonhienne TGA, Sagulenko E, Webb RI, Kee K-C, Franke J, Devos DP, Nouwens A, Carroll BJ, Fuerst JA (2010) Endocytosis-like protein uptake in the bacterium *Gemmata obscuriglobus*. Proc Natl Acad Sic USA 107:12883–12888

Luzzati V (1997) Biological significance of lipid polymorphism: the cubic phases. Curr Opin Struct Biol 7:661–668

Madani F, Lindberg S, Langel Ű, Futaki S, Gräslund A (2011) Mechanisms of cellular uptake of cell-penetrating peptides. J Biophysics 2011:414729

Magzoub M, Gräslund A (2004) Cell-penetrating peptides: small from inception to application. Q Rev Biophys 37:147–195

McLaughlin S, Murray D (2005) Plasma membrane phosphoinositide organization by protein electrostatics. Nature 438:605–611

Mishra A, Gordon VD, Yang L, Coridan R, Wong GCL (2008) HIV TAT forms pores in membranes by inducing saddle-spray curvature: potential role of bidentate hydrogen bonding. Angew Chem Int Ed 47: 2986–2989

Mishra A, Lai GH, Schmidt NW, Sun VZ, Rodriguez AR, Tong R, Tang L, Cheng J, Deming TJ, Kamei DT, Wong GCL (2011) Translocation of HIV TAT peptide and analogues induced by multiplexed membrane and cytoskeletal interactions. Proc Natl Acad Sci U S A 108:16883–16888

Moghal MMR, Islam MZ, Sharmin S, Levadnyy V, Moniruzzaman M, Yamazaki M (2018) Continuous detection of entry of cell-penetrating peptide transportan 10 into single vesicles. Chem Phys Lipids 212:120–129

Moniruzzaman M, Alam JM, Dohra H, Yamazaki M (2015) Antimicrobial peptide lactoferricin B-induced rapid leakage of internal contents from single giant unilamellar vesicles. Biochemistry 54:5802–5814

Moniruzzaman M, Islam MZ, Sharmin S, Dohra H, Yamazaki M (2017) Entry of a six-residue antimicrobial peptide derived from lactoferricin B into single vesicles and *Escherichia coli* cells without damaging their membranes. Biochemistry 56:4419–4431

Nekhotiaeva N, Elmquist A, Rajarao GK, Hällbrink M, Langel C, Good L (2004) Cell entry and antimicrobial properties of eukaryotic cell-penetrating peptides. FASEB J 18:394–396

Oka T, Tsuboi T, Saiki T, Takahashi T, Alam JM, Yamazaki M (2014) Initial step of pH-jump-induced lamellar to bicontinuous cubic phase transition in dioleoylphosphatidylserine/monoolein. Langmuir 30:8131–8140

Okamoto Y, Masum SM, Miyazawa H, Yamazaki M (2008) Low pH-induced transformation of bilayer membrane into bicontinuous cubic phase in dioleoyl-phosphatidylserine/monoolein membranes. Langmuir 24:3400–3406

Palm C, Netzereab S, Hällbrink M (2006) Quantitatively determined uptake of cell-penetrating peptides in non-mammalian cells with an evaluation of degradation and antimicrobial effects. Peptides 27:1710–1716

Persson D, Thorén PEG, Ksbjörner EK, Goksör M, Lincoln P, Nordén B (2004) Vesicles size-dependent translocation of penetratin analogs across lipid membranes. Biochim Biophys Acta 1665:142–155

Pisa MD, Chassaing G, Swiecicki J-M (2015) Translocation mechanism(s) of cell-penetrating peptides: biophysical studies using artificial membrane bilayers. Biochemistry 54:194–207

Pooga M, Hällbrink M, Zorko M, Langel Ű (1998) Cell penetration by transportan. FASEB J 12:67–77

Pooga M, Kut C, Kihlmark M, Hällbrink M, Fernaeus S, Raid R, Land T, Hallberg E, Bartfai TM, Langel Ű (2001) Cellular translocation of proteins by transportan. FASEB J 15:1451–1453

Qian Z, Dougherty PG, Pei D (2015) Monitoring the cytosolic entry of cell-penetrating peptides using a pH-sensitive fluorophore. Chem Commun 51:2162–2165

Qian Z, Martyna A, Hard RL, Wang J, Appiah-Kubi G, Coss C, Phelps MA, Rossman JS, Pei D (2016) Discovery and mechanism of highly efficient cyclic cell-penetrating peptides. Biochemistry 55:2601–2612

Rawictz W, Olbrich KC, McIntosh T, Needham D, Evans E (2000) Effect of chain length and unsaturation on elasticity of lipid bilayers. Biophys J 79:328–339

Richard JP, Melikov K, Vivès E, Ramos C, Verbeure B, Gait MJ, Chernomordik LV, Lebleu B (2003) Cell-penetrating peptides. A reevaluation of the mechanism of cellular uptake. J Biol Chem 278:585–590

Rothbard JB, Jessop TC, Wender PA (2005) Adaptive translocation: the role of hydrogen bonding and membrane potential in the uptake of guanidium-rich transporters into cells. Adv Drug Deliv Rev 57:495–504

Sandre O, Moreaux L, Brochard-Wyard F (1999) Dynamics of transient pores in stretched vesicles. Proc Natl Acad Sci U S A 96:10591–10596

Seddon JM, Templer RH (1995) Polymorphism of lipid-water systems. In: Lipowsky R, Sackmann E (eds) Structure and dynamics of membranes. Elsevier Science BV, Amsterdam, pp 97–160

Sharmin S, Islam MZ, Karal MAS, Shibly SUA, Dohra H, Yamazaki M (2016) Effects of lipid composition on the entry of cell-penetrating peptide oligoarginine into single vesicles. Biochemistry 55:4154–4165

Soomets U, Lindgren M, Gallet X, Pooga M, Hällbrink M, Elmquist A, Balaspiri L, Zorko M, Pooga M, Brasseur R, Langel Ű (2000) Deletion analogues of transportan. Biochim Biophys Acta 1467:165–176

Stanzl EG, Trantow BM, Vargas JR, Wender PA (2013) Fifteen years of cell-penetrating, guanidinium-rich molecular transporters: basic science, research tools, and clinical applications. Acc Chem Res 46:2944–2954

Sun D, Forsman J, Lund M, Woodward CE (2014) Effect of arginine-rich cell penetrating peptides on membrane pore formation and lifetimes: a molecular simulation study. Phys Chem Chem Phys 16:20785–20795

Sun D, Forsman J, Woodward CE (2015) Atomistic molecular simulations suggest a kinetic model for membrane translocation by arginine-rich peptides. J Phys Chem B 119:14413–14420

Swiecicki J-M, Bartsch A, Tailhades J, Di Pisa M, Heller B, Chassaing G, Mansuy C, Burlina F, Lavielle S (2014) The efficacies of cell-penetrating peptides in accumulating in large unilamellar vesicles depend on their ability to form inverted micelles. Chembiochem 15:884–891

Takechi Y, Yoshii H, Tanaka M, Kawakami T, Aimoto S, Saito H (2011) Physicochemical mechanism for the enhanced ability of lipid membrane penetration of polyarginine. Langmuir 27:7099–7107

Tamba Y, Yamazaki M (2005) Single giant unilamellar vesicle method reveals effect of antimicrobial peptide, magainin 2, on membrane permeability. Biochemistry 44:15823–15833

Tamba Y, Yamazaki M (2009) Magainin 2-induced pore formation in membrane depends on its concentration in membrane interface. J Phys Chem B 113:4846–4852

Tamba Y, Ohba S, Kubota M, Yoshioka H, Yoshioka H, Yamazaki M (2007) Single GUV method reveals interaction of Tea catechin (−)-epigallocatechin gallate with lipid membranes. Biophys J 92:3178–3194

Tamba Y, Ariyama H, Levadny V, Yamazaki M (2010) Kinetic pathway of antimicrobial peptide magainin 2-induced pore formation in lipid membranes. J Phys Chem B 114:12018–12026

Tanaka T, Sano R, Yamashita Y, Yamazaki M (2004) Shape changes and vesicle fission of giant unilamellar vesicles of liquid-ordered phase membrane induced by lysophosphatidylcholine. Langmuir 20:9526–9534

Ter-Avetisyan G, Tünnemann G, Nowak D, Nitschke M, Herrmann A, Drab M, Cardoso MC (2009) Cell entry of arginine-rich peptides is independent of endocytosis. J Biol Chem 284:3370–3378

Terrone D, Sang SLW, Roudaia L, Silvius JR (2003) Penetratin and related cell-penetrating cationic peptides can translocate across lipid bilayers in the presence of a transbilayer potential. Biochemistry 42:13787–13799

Thorén PEG, Persson D, Karlsson M, Nordén B (2000) The Antennapedia peptide penetratin translocates across lipid bilayers—the first direct observation. FEBS Lett 482:265–268

Thorén PEG, Persson D, Ksbjörner EK, Goksör M, Lincoln P, Nordén B (2004) Membrane binding and translocation of cell-penetrating peptides. Biochemistry 43:3471–3489

Vivès E, Brodin P, Lebleu B (1997) A truncated HIV-1 Tat protein basic domain rapidly translocates through the plasma membrane and accumulates in the cell nucleus. J Biol Chem 272:16010–16017

Wadia JS, Stan RV, Dowdy SE (2004) Transducible TAT-HA fusogenic peptide enhances escape of TAT-fusion proteins after lipid raft macropinocytosis. Nat Med 37:147–195

Walrant A, Matheron L, Cribier S, Chaignepain S, Jobin M-L, Sagan S, Alves ID (2013) Direct translocation of cell-penetrating peptides in liposomes: a combined mass spectrometry quantification and fluorescence detection study. Anal Biochem 438:1–10

Wang T-Y, Sun Y, Muthukrishnan N, Erazo-Oliveras A, Hajjar K, Pellois J-P (2016) Membrane oxidation enables the cytosolic entry of polyarginine cell-penetrating peptides. J Biol Chem 291:7902–7814

Wheaten SA, Ablan FDO, Spaller BL, Trieu JM, Almeida PF (2013) Translocation of cationic amphipathic peptides across the membranes of pure phospholipid giant vesicles. J Am Chem Soc 135:16517–16525

Wohlert J, den Otter WK, Edholm O, Briels WJ (2006) Free energy of a trans-membrane pore calculated from atomistic molecular dynamics simulations. J Chem Phys 124:154905

Yamazaki M (2008) The single GUV method to reveal elementary processes of leakage of internal contents from liposomes induced by antimicrobial substances. Adv Planar Lipid Bilayers Liposomes 7:121–142

Yamazaki M, Miyazu M, Asano T, Yuba A, Kume N (1994) Direct evidence of induction of interdigitated gel structure in large unilamellar vesicles of dipalmitoylphophatidylcholine by ethanol: studies by excimer method and high-resolution electron cyromicroscopy. Biophys J 66:729–733

Yandek LE, Pokomy A, Floren A, Knoeike K, Langel Ű, Almeida PFF (2007) Mechanism of the cell-penetrating peptide transportan 10 permeation of lipid bilayers. Biophys J 92:2434–2444

Yandek LE, Pokomy A, Almeida PFF (2008) Small changes in the primary structure of transportan 10 alter the thermodynamics and kinetics of its interaction with phospholipid vesicles. Biochemistry 47: 3051–3060

Yesylevskyy S, Marrink S-J, Mark AE (2009) Alternative mechanisms for the interaction of the cell-penetrating peptides penetratin and the TAT peptide with lipid bilayers. Biophys J 97:40–49

Zorko M, Langel Ű (2005) Cell-penetrating peptides: mechanism and kinetics of cargo delivery. Adv Drug Deliv Rev 57:529–545